Concordance of Disease Progression in Bilateral Geographic Atrophy Due to AMD

Monika Fleckenstein,[1,2] *Christine Adrion,*[2,3] *Steffen Schmitz-Valckenberg,*[1] *Arno P. Göbel,*[1] *Almut Bindewald-Wittich,*[1] *Hendrik P. N. Scholl,*[1] *Ulrich Mansmann,*[3] *and Frank G. Holz,*[1] *for the FAM Study Group*[4]

Purpose. To determine the degree of concordance for progression rate, size of atrophy, and visual acuity in patients with bilateral geographic atrophy (GA) due to age-related macular degeneration (AMD).

Methods. Analysis was performed in 156 eyes of 78 patients with bilateral GA. Best corrected visual acuity was determined with ETDRS charts. GA was quantified in digital fundus autofluorescence images (excitation, 488 nm; emission, >500 nm) by semiautomated imaging analysis. A linear, two-level, random-effects model was used to assess the natural course of disease. The concordance correlation coefficient (CCC) was calculated to assess the degree of agreement between disease characteristics of the left and right eyes. Bland-Altman plots were applied to compare measurements in the eyes.

Results. CCC between the eyes was 0.310 (95% CI, 0.097–0.495) for visual acuity, 0.706 (95% CI, 0.575–0.801) for GA size, and 0.756 (95% CI, 0.644–0.837) for GA progression rate. Although Bland-Altman plots revealed high concordance for the progression rate, there was considerable discrepancy between both eyes for GA.

Conclusions. GA progression in bilateral atrophic AMD is a symmetrical process; however, GA size may differ substantially between the eyes. High concordance in intraindividual disease progression in the presence of a high degree of interindividual variability indicates an influence by genetic and/or environmental factors rather than nonspecific ageing changes. The relatively small concordance of GA size in this cohort may indicate asymmetric evolution of the disease in affected individuals. The results may be useful in the design of future clinical trials designed to slow the rate of GA progression (Clinical Trials.gov number, NCT00393692). (*Invest Ophthalmol Vis Sci.* 2010;51:637–642) DOI:10.1167/iovs.09-3547

Age-related macular degeneration (AMD) is a complex disease with both genetic and environmental factors. It has become the most common cause of legal blindness in all industrialized countries.[1–8] Geographic atrophy (GA) occurs in the late-stage of dry AMD. It is the second most common cause of severe visual loss due to AMD, the most common being choroidal neovascularization. In individuals older than 85 years the prevalence of GA has recently been found to be four times higher than neovascular AMD. Studies suggest that 48% to 65% of prevalent cases involve bilateral GA.[9]

Because of severe visual loss in advanced AMD, the public health impact, burden of illness, and secondary costs are significant. Several studies have shown that AMD can severely impair quality of life and that increasing vision loss is associated with increasing impairment of quality of life and frequently causes depression.[10]

GA is characterized by the development and gradual enlargement of uni- or multifocal atrophic patches that involve the retinal pigment epithelium as well as the corresponding neurosensory retina and choriocapillaris layer of the choroid.[11,12] Areas of GA therefore correspond to absolute scotomas.[11] Despite the recent breakthrough with anti-VEGF therapy for neovascular AMD, there is still no treatment available for patients with GA and no means to prevent or slow the progressive visual impairment. To develop new therapeutic interventions, a better understanding of the natural history and the underlying disease process appears mandatory.

Natural history studies have addressed various disease characteristics of GA, including progression rates and functional impact.[9,11,13–19] Scanning laser ophthalmoscopy (SLO) allowing for detection of abnormal fundus autofluorescence (FAF) has recently been introduced to detect and accurately delineate GA areas. Furthermore, it identifies predictive markers for disease progression based on perilesional patterns of abnormal FAF.[16,18,20–22] These findings also indicate a role of excessive lipofuscin accumulation in the retinal pigment epithelium (RPE) and toxic fluorophores such as A2-E (*N*-retinylidene-*N*-retinylethanol-amine) in the pathogenesis of outer retinal atrophy in the context of AMD.

Previous natural history studies have found considerable variability among patients with GA with regard to configuration, size, number, and spread of atrophic patches.[9,12,14–16,19,23,24] In patients with bilateral GA, we have demonstrated a high degree of symmetry of FAF patterns between the eyes of a patient in the presence of extensive interindividual variability.[24] Furthermore, a positive correlation of size and configuration of atrophic patches and progression rates has been reported,[15,19,24,25] whereas the correlation of visual acuity between the eyes was less pronounced.[9]

From the [1]Department of Ophthalmology, University of Bonn, Bonn, Germany; and the [3]Department of Medical Informatics, Biometry and Epidemiology, Ludwig-Maximilians University, Munich, Germany.

[2]Contributed equally to the work and therefore should be considered equal authors.

[4]Study Group members are listed in the Appendix.

Supported by DFG (German Research Council) Research Priority Program Age-Related Macular Degeneration Grant SPP 1088, Ho 1926/1-3; EU FP6; Integrated Project EVI-GENORET (LSHG-CT-2005-512036); a DOG (German Society of Ophthalmology) research grant; and BONFOR Program Grant O-137-0012 to the Faculty of Medicine, University of Bonn.

Submitted for publication February 10, 2009; revised June 1 and July 26, 2009; accepted September 1, 2009.

Disclosure: **M. Fleckenstein**, Heidelberg Engineering (F); **C. Adrion**, Heidelberg Engineering (F); **S. Schmitz-Valckenberg**, Heidelberg Engineering (F); **A.P. Göbel**, Heidelberg Engineering (F); **A. Bindewald-Wittich**, Heidelberg Engineering (F); **H.P.N. Scholl**, Heidelberg Engineering (F); **U. Mansmann**, Heidelberg Engineering (F); **F.G. Holz**, Heidelberg Engineering (F, C)

Corresponding author: Frank G. Holz, Department of Ophthalmology, University of Bonn, Ernst-Abbe-Str. 2, D-53127 Bonn, Germany; frank.holz@ukb.uni-bonn.de.

Although widely used, the calculation of standard correlation coefficients appears to be an inappropriate method of evaluating the concordance of disease characteristics for a paired organ and therefore does not reflect the degree of symmetry in bilateral GA. Although good correlation implies the possibility of calibrating two measurements by a linear relationship, concordance requires a stricter definition of calibration (i.e., identity).[26]

The purpose of this study was to determine in a large cohort of patients with GA the concordance between the eyes with respect to visual acuity, GA size, and progression rate.

Methods

Study Population

Patients with bilateral uni- and/or multifocal GA and at least two examinations of each eye with sufficient image quality to accurately determine the size of atrophy were included from the GA arm of the longitudinal natural history multicenter FAM (Fundus Autofluorescence in age-related Macular Degeneration) Study. Diagnosis was initially made funduscopically when atrophy was visible in eyes with AMD and when there were no clinical signs of concomitant CNV. The presence of GA was confirmed by FAF imaging, whereby atrophic lesions show a well-defined area of markedly decreased FAF signal due to the absence of RPE cells and, thus, lipofuscin, the molecular constituents of which include the dominant fluorophores identified by FAF imaging. The study adhered to the tenets of the Declaration of Helsinki and was approved by the local institutional review boards and the ethics committees at the participating study centers. Informed consent was obtained from each patient after explanation of the nature and possible consequences of the study.

Exclusion criteria included any history of neovascular AMD, retinal surgery, laser photocoagulation, and radiation therapy or other retinal diseases in either eye. Best corrected visual acuity (BCVA) in logMAR was determined with Early Treatment Diabetic Retinopathy Study (ETDRS) charts on a quasi-logarithmic ordinal scale. Before examination, the pupil of the study eye was dilated with 1% tropicamide eye drops. A standardized case report form (CRF) including ophthalmic history, possible risk factors, and family history was completed for each patient.[16–18,27]

Image Acquisition and Processing

FAF was recorded with one of two confocal scanning laser ophthalmoscopes (cSLO; the Heidelberg Retina Angiographs HRA classic and HRA 2; Heidelberg Engineering, Heidelberg, Germany), the optical and technical principles of which have been described previously.[28–30] FAF images were recorded in accordance to a standard operation procedure (SOP) including focusing in the red-free reflection mode ($\lambda = 514$ nm for HRA classic, $\lambda = 488$ nm for HRA 2), acquisition of a series of $30° \times 30°$ images (488 nm), and calculation of mean images after automated alignment (of nine single images) to amplify signal-to-noise ratio with image analysis software (Heidelberg Eye Explorer; Heidelberg Engineering).[17] The image resolution was 512×512 pixels for the HRA classic and 768×768 pixels for the HRA 2.

Further improving our previous image analysis,[16,31] serial FAF images of the same eye were processed by using image-analysis software (Picture Window Pro 4.0.1.2 analysis software; Digital Light & Color, Cambridge, MA). Four points—anatomic landmarks surrounding the atrophic area such as bifurcations of blood vessel—were selected in each serial image of an eye, and the four-point-alignment function was applied whereby the respective overlay image was shifted, rotated, scaled, and warped so that all four corresponding points were congruent in serial images. The total size of GA was measured in the processed FAF images by automated image-analysis software that uses region-growing techniques to segment the areas of GA.[32,33]

Statistical Methods

Statistical analyses included frequency and descriptive statistics. The Spearman rank correlation coefficient (ρ)[34] was applied as a nonparametric measure of correlation to assess whether there is a monotonic relationship between two disease characteristics. The significance level was set to 5%. A linear mixed effects model[35–37] was used to quantify overall (long-term) GA growth. A detailed description of the longitudinal modeling process is given elsewhere.[31] The two-level, random-effects model separates eye-specific and patient-specific effects and helps to analyze related observations. The mixed model methodology allows analysis of variance components and fixed effects simultaneously. A random intercept as well as a random slope for "patient" and "eye within patient" was introduced to account for unexplained heterogeneity.

The concordance correlation coefficient (CCC) was used to evaluate the degree of agreement of measurements obtained for the left and right eyes in patients with bilateral GA.[38,39] The CCC herein can be interpreted as extent of symmetry. The CCC combines measures of both precision and accuracy, to determine how far the observed data deviate from the line of perfect concordance (that is, the line at 45° on a square scatterplot on which all points would lie if measurements of both eyes were exactly the same).

The value of the concordance correlation coefficient is scaled between −1 and 1, and evaluates the degree to which pairs fall on the 45° line (CCC = 1) or −45° line (CCC = −1). A CCC of 1 is total agreement, 0 is no agreement at all, −1 is an inverse total agreement. However, the extent of the confidence interval has to be taken into account for the interpretation. Lin's CCC increases in value as a function of the nearness of the data's reduced major axis to the line of perfect concordance (the accuracy of the data) and of the tightness of the data about its reduced major axis (the precision of the data).

Furthermore, graphic techniques were applied. The degree of intraindividual agreement (concordance) was assessed according to the descriptive method of Bland and Altman.[26] For each patient, the differences between measurements (i.e., GA size, GA progression rate, and visual acuity) of both eyes as well as the mean of these two measurements were calculated. A difference of 0 indicates perfect agreement. The so-called limits of agreement are defined as the mean difference ± 2 SD (observed SD of the difference between the two measurements per patient).

The Bland-Altman plots of differences against means also determine any possible relationship between the variation within patients and the patient's average measurement.

In contrast to the CCC, the Bland-Altman plot is primarily a graphic approach to assessing the magnitude of disagreement (both error and bias), spotting outliers, and seeing whether there is any trend, for example an increase in differences (left minus right eye) for high mean values of both eyes.

The analysis of concordance of the GA size and visual acuity between the eyes of a patient was based on values obtained at the first time point when data were available for both eyes (measurements are taken at the same calendar time).

All statistical calculations were performed using the R software package version 2.7.0 (www.r-project.org) and commercial software (SAS 9.1.3; SAS Institute, Cary, NC). The R-library nonlinear mixed effects (NLME) function was used for longitudinal modeling.[40] The fit of different nested hierarchical models was assessed by means of a likelihood-ratio test.

Results

A total of 78 patients (156 eyes) with bilateral GA (47 women, 31 men) met the inclusion criteria. The median age at baseline examination was 73.5 years, with a range of 53 to 89 years. The median age at onset was 71 years, range 50 to 84 years (in 15.3% of cases, no data were available). Age at onset was defined as either the patient's age at which visual impairment was first noted or the age when the diagnosis was made. A total of 541 FAF images were suitable for quantifying GA size. The median follow-up period was 1.94 years (IQR, 0.96–3.37 years), with 76 eyes (41 patients) having equal or greater than

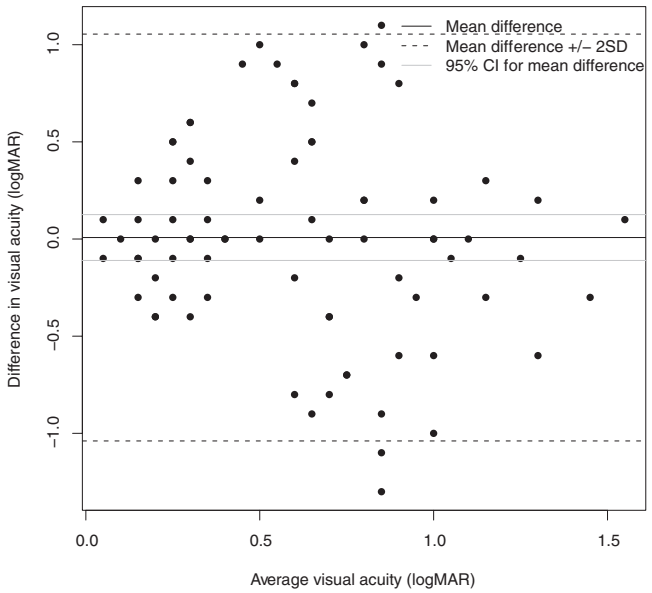

FIGURE 1. A Bland-Altman plot of visual acuity data: Difference (left eye minus right eye) against the mean of each pair of measurements for the eyes. *Top* and *bottom lines*: 95% limits of agreement (mean difference ± 2 SD of the differences). *Gray lines*: 95% CI for mean difference, 0.008 logMAR (−0.110 to 0.126 logMAR).

2 years' review period. In 21 patients, the follow-up period differed between the eyes, because of insufficient image quality either at the beginning or the end of the observation period in 20 patients. One patient had early AMD at first examination, with GA developing during the observational period.

The population mean growth rate was estimated to be 1.65 mm^2/year (95% CI, 1.45–1.86). The interindividual variability of the slope was 0.75 (95% CI, 0.60–0.94), whereas the variability of the slope within the eyes of a patient (intraindividual variability) was 0.50 (95% CI, 0.39–0.64). Measurement error indicating the remaining variability not explained by the model was 0.49 mm^2/year (95% CI, 0.45–0.54).

Analysis of concordance of the GA size and visual acuity between the eyes of a patient was based on values obtained at the first time point when data were available for both eyes.

Median visual acuity was 0.9 logMAR (interquartile range [IQR], 0.4–1.1), and the median size of GA was 8.93 mm^2 (IQR, 5.59–13.51 mm^2; range, 0.054–41.04).

Concordance of Visual Acuity

The absolute value of the differences between the eyes in visual acuity was 0.4 logMAR (mean). The CCC for visual acuity was 0.310 (95% CI, 0.097–0.495) indicating poor agreement between the eyes. Likewise, the Bland-Altman plot (Fig. 1) displayed considerable lack of concordance for visual acuity between the left and the right eye, with discrepancies of up to 1 logMAR. Thus, there was evidence of a relevant intraindividual variation in visual acuity.

Concordance of GA Size

Analysis of GA size revealed a significant positive correlation between the eyes (Spearman coefficient, $\rho = 0.592$; $P < 0.0001$). The median difference of the size of GA between the eyes did not differ significantly from 0 ($P = 0.403$, Wilcoxon-signed rank test). The absolute value of the difference in GA size between the eyes size was 3.36 mm^2 (mean).

The CCC was 0.706 (95% CI, 0.575–0.801), indicating a moderate to good degree of agreement in GA size between the eyes.

A Bland-Altman plot (Fig. 2) compared the mean GA size of all 78 measured pairs with the difference in measurements between the eyes and revealed a considerable discrepancy in GA size between the eyes, with discrepancies up to 10 mm^2.

With increasing average size of atrophic lesions the agreement declined and increased again with higher average GA size.

One patient was clearly an outlier, with a baseline GA size of 34.57 mm^2 in the left eye and 33.02 mm^2 in the right eye. As this outlier artificially tends toward the 45° line (i.e., the line of perfect agreement), the CCC was calculated without it, yielding in a CCC of 0.615 (95% CI, 0.456–0.736). When the outlier patient was included, the CCC was 0.706 (95% CI, 0.575–0.801). Hence, the extent of symmetry was rather moderate for GA size. The width of the confidence interval for CCC supports this finding. Figure 3 illustrates that GA size may differ between the eyes of a patient.

Concordance of GA Progression Rate

There was a significant correlation in the progression rate between the right and the left eye (Spearman-coefficient was $\rho = 0.74$; $P < 0.0001$). The median difference in the progression rate between the eyes did not differ significantly from 0 ($P = 0.369$, Wilcoxon signed rank test). The absolute value of the differences in GA progression rate between right and left eye was 0.42 mm^2/year (mean).

The CCC for agreement of the progression rate between the eyes was 0.756 (95% CI, 0.644–0.837) indicating a substantial intraindividual concordance of the GA progression rate. Figure 4 plots the differences between the two measurements per patient against the mean of the two measurements. The mean difference was −0.084 mm^2/year. The limits of agreement, ranging from −1.271 to 1.102, suggested a high intraindividual concordance in GA progression rate; however, in a few patients the progression rates of the eyes differed substantially. Figure 5 illustrates similar progression of GA in both eyes of a patient although there is marked difference in GA size.

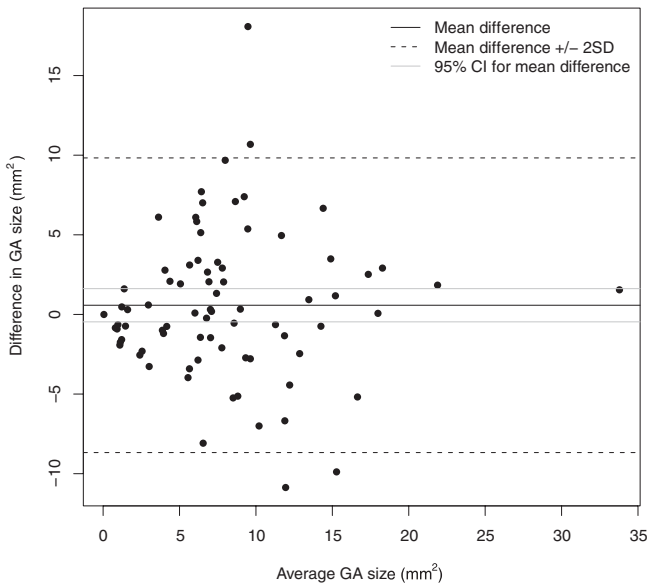

FIGURE 2. A Bland-Altman plot of GA size. Difference (left eye minus right eye) against the mean of each pair of measurements for the eyes. *Solid line*: mean difference; *top* and *bottom lines*: 95% limits of agreement (mean difference ± 2 SD of the differences). *Gray lines*: 95% CI for mean difference 0.577 mm^2 (−0.466 to 1.620 mm^2).

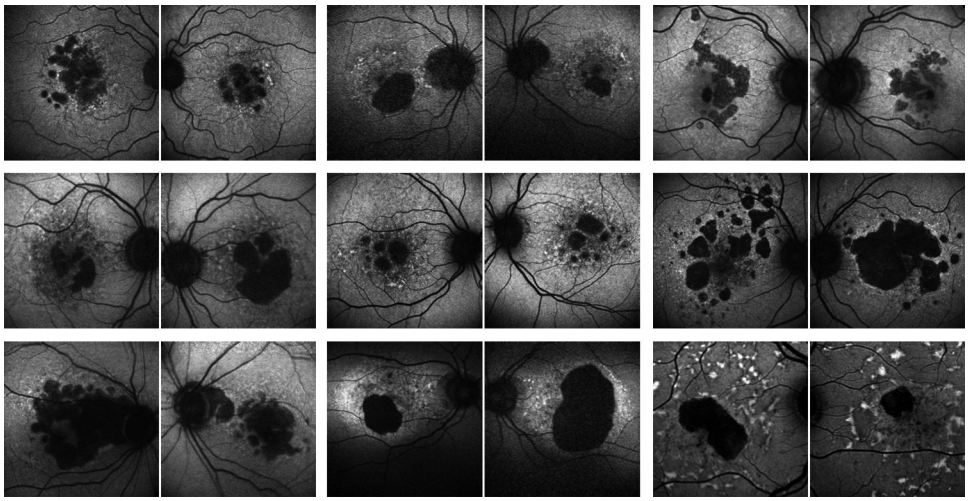

FIGURE 3. Fundus autofluorescence images of patients with bilateral geographic atrophy (images of the eyes are taken at the same time point). The images reflect that the size of GA may have differed between the eyes of a patient. However, there was a high degree of symmetry in the fundus autofluorescence pattern in the perilesional zone of GA and configuration of atrophy, whereas there was a high degree of interindividual variability.

DISCUSSION

This study demonstrates variable degrees of concordance of disease characteristics in patients with bilateral GA due to AMD. The CCC for agreement between both eyes was 0.310 for visual acuity, 0.706 for GA size, and 0.756 for GA progression. Comparing the measurements in the eyes by Bland-Altman plots, there was a high degree of concordance of GA progression but considerable discrepancy in GA size. These results indicate that, although the size of GA may differ substantially between the eyes of patients with bilateral GA, the progression rate represents a symmetrical process.

In previous studies addressing the degree of concordance in visual acuity, GA size, and GA progression rate, respectively, standard correlation coefficients were applied: Sunness et al.[15] reported a correlation coefficient of 0.81 for total baseline GA size in 83 patients with bilateral GA. In 62 patients with 2-year follow-up, the correlation coefficient was 0.76 for the progression rate with 36 of these patients having a difference in progression rate between the eyes of 0.6 mm^2/year or less. In addition, little correlation between the eyes was found in baseline visual acuity ($r = 0.18$), for visual acuity at 2 years ($r = 0.04$), and for a 2-year change in visual acuity ($r = 0.28$).[9] Overall differences in visual acuity between eyes were explained by differences in foveal involvement in the eyes. In addition, suboptimal use of the worse-seeing eye was considered.[9]

Klein et al.[19] reported a correlation coefficient of 0.87 for total GA size between eyes in 42 right-left eye pairs with bilateral GA. For 12 instances where both the right and the left eye had a 5-year change in data, the correlation coefficient between eyes was 0.85 for GA progression.

The results of these studies indicate a positive correlation in GA size and progression rate between both eyes in the presence of bilateral GA. However, standard correlation coefficients are not tailored to address the concordance between two phenotypic variables.[26] For instance, data that apparently seem to be in poor agreement can produce fairly high correlations. Therefore, the

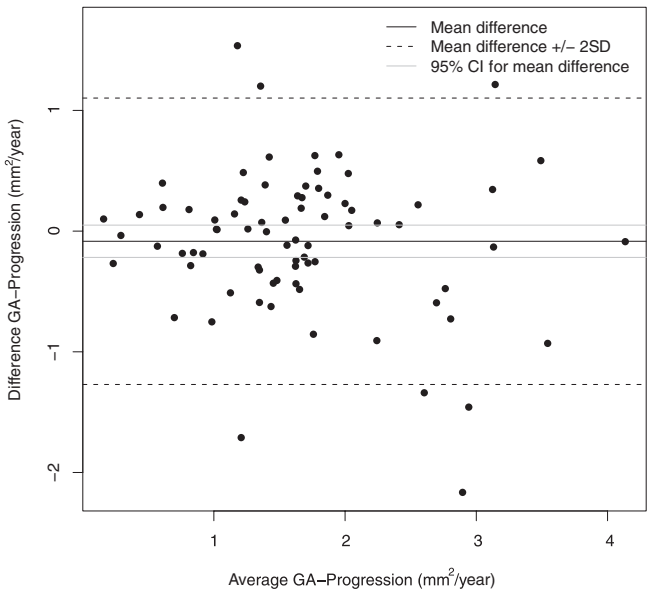

FIGURE 4. A Bland-Altman plot of GA progression rate data. Difference (left eye minus right eye) against the mean of each pair of measurements for the eyes. *Top* and *bottom lines*: 95% limits of agreement (mean difference, ±2 SD of the differences). *Gray lines*: 95% CI for mean difference −0.084 mm^2/y (−0.218 to 0.050 mm^2/year).

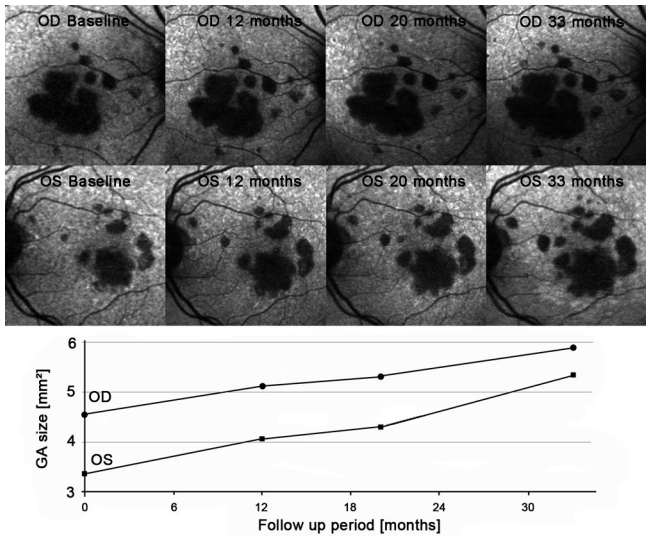

FIGURE 5. There was similar progression of GA in both eyes of a patient, although there was a marked difference in GA size. Serial FAF imaging in a patient with bilateral GA. GA size enlarged over time (follow-up period, 33 months). There was a marked difference in the size of GA between right (OD) and left eye (OS) at all examination dates. The progression rate (PR) in both eyes was relatively slow (PR OD, 0.51 mm^2/y versus PR OS, 0.71 mm^2/y; population mean PR: 1.65 mm^2/year, 95% CI, 1.45–1.86) and did not differ substantially between both eyes.

correlation coefficient is not a measure of agreement; it is a measure of association. Thus, high correlation of disease characteristics (e.g., GA size) between the eyes does not necessarily reflect a high degree of symmetry. This finding is easily seen when considering several pairs of measurements where one component differs from the second by a fixed amount what results in a high correlation but no symmetry. More suitable statistical approaches are CCC and Bland-Altman plots. The latter is a powerful way to assess the magnitude of disagreement (both error and bias), to detect outliers, and to see whether there is any trend (e.g., an increase in difference between intraindividual disease characteristics for high average values). By applying these statistical methods in our cohort, we found considerable discrepancy with respect to GA size. This observation may reflect different disease stages between fellow eyes. Since standard correlation coefficients were used in other studies, we do not know whether this observation would also be found in other cohorts of patients with bilateral GA.

The Bland-Altman plot revealed that with increasing average size of atrophic lesions, the agreement declined and increased again with higher average GA size. However, this observation could be an artifact of the construction of the mean: if the eyes both have small areas, or both have large areas, the average GA size would be small or large, respectively. The middle average GA size points might include patients with middle areas in both eyes as well as patients with small area in one eye and large in the other. This results in a higher variation for difference in GA values.

Although the size of GA between both eyes could differ substantially, there was a high degree of intraindividual symmetry in GA progression rate, which may indicate that specific disease mechanisms determine progression once GA has started. Although there was a high variability of disease progression among patients,[9,14–16,19] genetic and/or environmental factors rather than nonspecific ageing processes may be considered as determinants for the rate of progression.

Potential risk factors on GA progression have been addressed in previous studies. Age, hypertension, diabetes, smoking history, or body mass index had no impact on enlargement rates of GA in previous studies.[9,16,19] Although risk-variants of *CFH*, *C3*, and *ARMS2* confer susceptibility for all AMD disease phenotypes including GA,[41–43] a recent analysis showed that the risk alleles are not associated with GA progression over time.[44]

It has been shown that the GA progression rate is fairly constant over time. Sunness et al.[15] reported that knowledge of prior enlargement rate is predictive of subsequent enlargement rate. Furthermore, eyes with small areas tend to have a lower rate of enlargement compared to eyes with larger areas of GA.[9,15,16] However, the dependence of the progression rate on the baseline size of GA was found to be less strong than the dependence on the prior progression rate. Sunness et al.[15] also found a significant difference of the progression rate between patients with bilateral GA (mean, 2.6 mm^2/y) and patients with drusen in the fellow eye (mean, 1.3 mm^2/y); however, this difference was attributable to the lower baseline area in the fellow eye drusen group.[15]

A similar observation follows from our model[31] where the interindividual variability for the progression rate is larger than the intraindividual variability between both eyes. Therefore, a low individual progression rate will persist for both eyes. Similar results hold for a higher progression rate. The deviation of the individual progression rate from the population mean rate will persist and determine the individual course of the disease.

Recently, we reported that distinct abnormal perilesional FAF patterns have an impact on disease progression in eyes with GA and, therefore, serve as prognostic determinants.[16] Furthermore, high symmetry of these FAF patterns between fellow eyes has been demonstrated in the presence of a high variability between patients.[24] These findings support the assumption that individual characteristics define the GA phenotype and that variability between patients reflect heterogeneity on the cellular and molecular level.

The high concordance of atrophy progression rates is relevant for the design of interventional trials in patients with GA to slow down enlargement of atrophic areas. By including only patients with bilateral GA and assigning the untreated eye as the control if a topical administration is used, the required sample size may be significantly reduced with unilateral treatment.[14,15]

Certain limitations have to be considered for this study. The follow-up period was variable among the patients, with a median period of 1.94 years. Within patients, follow-up of the left and the right eyes could also differ due to insufficient image quality for GA measurement in one eye at the beginning or end of the observation period ($n = 20$) or due to GA development in one eye between examination dates ($n = 1$). The sample size of examined patients was relatively small. However, the FAM study represents the largest cohort of GA patients with cSLO-FAF imaging and prospective longitudinal examinations. All area measurements were performed in FAF images which represent an accurate way of quantifying atrophic patches in the human eye. The image-acquisition and grading protocols used herein[27,32,45] have been established by the GRADE Reading Center Bonn, University of Bonn, Germany (http://www.augenklinik.uni-bonn.de/grade).

In conclusion, the results indicate that GA spread in bilateral late atrophic AMD is a highly symmetrical process. Discrepancy in GA size may reflect an asymmetric onset of atrophic disease in affected individuals. A high degree of concordance in intraindividual disease progression in the presence of a high degree of interindividual variability would indicate an influence by individual characteristics rather than nonspecific ageing changes.

References

1. Ambati J, Ambati BK, Yoo SH, Ianchulev S, Adamis AP. Age-related macular degeneration: etiology, pathogenesis, and therapeutic strategies. *Surv Ophthalmol.* 2003;48:257–293.
2. Chakravarthy U, Augood C, Bentham GC, et al. Cigarette smoking and age-related macular degeneration in the EUREYE Study. *Ophthalmology.* 2007;114:1157–1163.
3. Klaver CC, Wolfs RC, Vingerling JR, Hofman A, de Jong PT. Age-specific prevalence and causes of blindness and visual impairment in an older population: the Rotterdam Study. *Arch Ophthalmol.* 1998;116:653–658.
4. Klein R, Klein BE, Knudtson MD, et al. Fifteen-year cumulative incidence of age-related macular degeneration: the Beaver Dam Eye Study. *Ophthalmology.* 2007;114:253–262.
5. Tomany SC, Wang JJ, Van LR, et al. Risk factors for incident age-related macular degeneration: pooled findings from 3 continents. *Ophthalmology.* 2004;111:1280–1287.
6. van Leeuwen R, Klaver CC, Vingerling JR, Hofman A, de Jong PT. Epidemiology of age-related maculopathy: a review. *Eur J Epidemiol.* 2003;18:845–854.
7. Wang JJ, Rochtchina E, Lee AJ, et al. Ten-year incidence and progression of age-related maculopathy: the blue Mountains Eye Study. *Ophthalmology.* 2007;114:92–98.
8. Augood CA, Vingerling JR, de Jong PT, et al. Prevalence of age-related maculopathy in older Europeans: the European Eye Study (EUREYE). *Arch Ophthalmol.* 2006;124:529–535.
9. Sunness JS, Gonzalez-Baron J, Applegate CA, et al. Enlargement of atrophy and visual acuity loss in the geographic atrophy form of age-related macular degeneration. *Ophthalmology.* 1999;106:1768–1779.
10. Slakter JS, Stur M. Quality of life in patients with age-related macular degeneration: impact of the condition and benefits of treatment. *Surv Ophthalmol.* 2005;50:263–273.
11. Sunness JS. The natural history of geographic atrophy, the advanced atrophic form of age-related macular degeneration. *Mol Vis.* 1999;5:25.

12. Sarks JP, Sarks SH, Killingsworth MC. Evolution of geographic atrophy of the retinal pigment epithelium. *Eye.* 1988;2:552–577.
13. Sunness JS, Rubin GS, Applegate CA, et al. Visual function abnormalities and prognosis in eyes with age-related geographic atrophy of the macula and good visual acuity. *Ophthalmology.* 1997;104: 1677–1691.
14. Sunness JS, Applegate CA, Bressler NM, Hawkins BS. Designing clinical trials for age-related geographic atrophy of the macula: enrollment data from the geographic atrophy natural history study. *Retina.* 2007;27:204–210.
15. Sunness JS, Margalit E, Srikumaran D, et al. The long-term natural history of geographic atrophy from age-related macular degeneration: enlargement of atrophy and implications for interventional clinical trials. *Ophthalmology.* 2007;114:271–277.
16. Holz FG, Bindewald-Wittich A, Fleckenstein M, et al. Progression of geographic atrophy and impact of fundus autofluorescence patterns in age-related macular degeneration. *Am J Ophthalmol.* 2007;143:463–472.
17. Schmitz-Valckenberg S, Bultmann S, Dreyhaupt J, et al. Fundus autofluorescence and fundus perimetry in the junctional zone of geographic atrophy in patients with age-related macular degeneration. *Invest Ophthalmol Vis Sci.* 2004;45:4470–4476.
18. Schmitz-Valckenberg S, Bindewald-Wittich A, Dolar-Szczasny J, et al. Correlation between the area of increased autofluorescence surrounding geographic atrophy and disease progression in patients with AMD. *Invest Ophthalmol Vis Sci.* 2006;47:2648–2654.
19. Klein R, Meuer SM, Knudtson MD, Klein BE. The epidemiology of progression of pure geographic atrophy: The Beaver Dam Eye Study. *Am J Ophthalmol.* 2008.
20. Holz FG, Bellmann C, Staudt S, Schütt F, Völcker HE. Fundus autofluorescence and development of geographic atrophy in age-related macular degeneration. *Invest Ophthalmol Vis Sci.* 2001;42:1051–1056.
21. Holz FG, Pauleikhoff D, Klein R, Bird AC. Pathogenesis of lesions in late age-related macular disease. *Am J Ophthalmol.* 2004;137: 504–510.
22. Lois N, Owens SL, Coco R, et al. Fundus autofluorescence in patients with age-related macular degeneration and high risk of visual loss. *Am J Ophthalmol.* 2002;133:341–349.
23. Maguire P, Vine AK. Geographic atrophy of the retinal pigment epithelium. *Am J Ophthalmol.* 1986;102:621–625.
24. Bellmann C, Jorzik J, Spital G, et al. Symmetry of bilateral lesions in geographic atrophy in patients with age-related macular degeneration 1. *Arch Ophthalmol.* 2002;120:579–584.
25. Schatz H, McDonald HR. Atrophic macular degeneration: rate of spread of geographic atrophy and visual loss. *Ophthalmology.* 1989;96:1541–1551.
26. Bland JM, Altman DG. Statistical methods for assessing agreement between two methods of clinical measurement. *Lancet.* 1986;1: 307–310.
27. Bindewald A, Schmitz-Valckenberg S, Jorzik JJ, et al. Classification of abnormal fundus autofluorescence patterns in the junctional zone of geographic atrophy in patients with age related macular degeneration. *Br J Ophthalmol.* 2005;89:874–878.
28. Bindewald A, Jorzik JJ, Roth F, Holz FG. cSLO digital fundus autofluorescence imaging (in German). *Ophthalmologe.* 2005;102: 259–264.
29. Holz FG, Bellmann C, Rohrschneider K, Burk RO, Volcker HE. Simultaneous confocal scanning laser fluorescein and indocyanine green angiography. *Am J Ophthalmol.* 1998;125:227–236.
30. Jorzik JJ, Bindewald A, Dithmar S, Holz FG. Digital simultaneous fluorescein and indocyanine green angiography, autofluorescence, and red-free imaging with a solid-state laser-based confocal scanning laser ophthalmoscope. *Retina.* 2005;25:405–416.
31. Dreyhaupt J, Mansmann U, Pritsch M, et al. Modelling the natural history of geographic atrophy in patients with age-related macular degeneration. *Ophthalmic Epidemiol.* 2005;12:353–362.
32. Deckert A, Schmitz-Valckenberg S, Jorzik J, et al. Automated analysis of digital fundus autofluorescence images of geographic atrophy in advanced age-related macular degeneration using confocal scanning laser ophthalmoscopy (cSLO). *BMC Ophthalmol.* 2005;5:8.
33. Schmitz-Valckenberg S, Jorzik J, Unnebrink K, Holz FG. Analysis of digital scanning laser ophthalmoscopy fundus autofluorescence images of geographic atrophy in advanced age-related macular degeneration 3. *Graefes Arch Clin Exp Ophthalmol.* 2002;240:73–78.
34. Altman DG. *Practical Statistics for Medical Research.* London: Chapman & Hall; 1991.
35. Pinheiro JC, Bates DM. *Mixed-Effects Models in S and S-PLUS.* Berlin: Springer Statistics and Computing; 2000.
36. Verbeke G, Molenberghs G. *Linear Mixed Models for Longitudinal Data.* New York: Springer; 2000.
37. Weiss RE. *Modeling Longitudinal Data.* New York: Springer; 2005.
38. Lin LI. A concordance correlation coefficient to evaluate reproducibility. *Biometrics.* 1989;45:255–268.
39. Lin L. Overview of agreement statistics for medical devices. *J Biopharm Stat.* 2008;18:126–144.
40. R Development Core Team. *R: A Language and Environment for Statistical Computing*. Vienna, Austria: R Foundation for Statistical Computing; 2007.
41. Maller JB, Fagerness JA, Reynolds RC, et al. Variation in complement factor 3 is associated with risk of age-related macular degeneration. *Nat Genet.* 2007;39:1200–1201.
42. Schaumberg DA, Hankinson SE, Guo Q, Rimm E, Hunter DJ. A prospective study of 2 major age-related macular degeneration susceptibility alleles and interactions with modifiable risk factors. *Arch Ophthalmol.* 2007;125:55–62.
43. Yates JR, Sepp T, Matharu BK, et al. Complement C3 variant and the risk of age-related macular degeneration. *N Engl J Med.* 2007; 357:553–561.
44. Scholl HP, Fleckenstein M, Fritsche LG, et al. CFH, C3 and ARMS2 are significant risk loci for susceptibility but not for disease progression of geographic atrophy due to AMD. *PLoS One*. 2009; 4(10):e7418.
45. Göbel AP, Schmitz-Valckenberg S, Fleckenstein M, et al. Quantification of areas of geographic atrophy due to AMD in longitudinal digital cSLO fundus autofluorescence images (Abstract). German Ophthalmological Society, 2007.

Appendix

FAM Study Group

Department of Ophthalmology, *University of Bonn*, *Bonn*, *Germany*: Frank G. Holz, Hendrik P. N. Scholl, Monika Fleckenstein, Steffen Schmitz-Valckenberg, Almut Bindewald-Wittich, Arno P. Göbel, Kerstin Bartsch, and Martina Hofmann.

Department of Medical Informatics, *Biometry and Epidemiology*, *Ludwig-Maximilians-University*, *Munich*: Ulrich Mansmann, Christine Adrion, and Ladan Baghi.

Department of Ophthalmology, *University of Aachen*, *Aachen*, *Germany*: Peter Walter, Andreas Weinberger, and Cordula Eddahabi.

Department of Ophthalmology, *Inselspital*, *University of Bern*, *Bern*, *Switzerland*: Sebastian Wolf, Wilma Einbock, and Ute Wolf-Schnurrbusch.

Department of Ophthalmology, *University of Heidelberg*, *Heidelberg*, *Germany*: Hans E Völcker, Matthias D. Becker, Stefan Dithmar, Friedericke Mackensen, Florian Schütt, Jörg J. Jorzik, Helena Sieber, and Maria Herrmann

Department of Medical Biometrics, *University of Heidelberg*, *Heidelberg*, *Germany*: Norbert Victor, Jens Dreyhaupt, and Andreas Deckert.

Department of Ophthalmology, *University of Leipzig*, *Leipzig*, *Germany*: Peter Wiedemann, Christian Foja, and Andreas Mössner.

Department of Ophthalmology, *St. Franziskus Hospital*, *Münster*, *Germany*: Daniel Pauleikhoff, Georg Spital, and Andrea Koschinski.

Department of Ophthalmology, *University of Würzburg*, *Würzburg*, *Germany*: Claudia v. Strachwitz